Int. J. Electrochem. Sci., 15 **(2020)** 11886 – 11903, doi: 10.20964/2020.12.07

International Journal of
ELECTROCHEMICAL
SCIENCE
www.electrochemsci.org

K_2NiF_4-type $La_{1.8}Sr_{0.2}CuO_4$ Cathode for Magnesium-air Battery

Tong Xue[1,#,*] , *Xiao-Lei Qiao*[1], *Jin-Fu Ma*[1], *Xiang-Hui Yan*[1], *Rui Lv*[1], *Feng-Lan Han*[1,2]

[1] School of Materials Science and Engineering, North Minzu University, Yinchuan, 750021, P.R.China.
[2] Collaborative Innovation Center for High Value Utilization of Industrial By-products, North Minzu University, Yinchuan, 750021, P.R.China.
[*]E-mail: tong_xue@nun.edu.cn

Received: 7 May 2019 / *Accepted:* 22 July 2020 / *Published:* 31 October 2020

In this study, the K_2NiF_4-type $La_{1.8}Sr_{0.2}CuO_4$ has been hydrothermal synthesized and applied in Mg-air battery. The hydrothermal time and heat treatment temperature of synthesized $La_{1.8}Sr_{0.2}CuO_4$ has been discussed. X-ray diffraction (XRD) and scanning electron spectroscopy (SEM) were carried out to demonstrate the crystalline structure and morphology of synthesized materials. The electrochemical impedance and discharge performance were studied to understand the catalytic activities of $La_{1.8}Sr_{0.2}CuO_4$. The $La_{1.8}Sr_{0.2}CuO_4$ with active carbon addition ($La_{1.8}Sr_{0.2}CuO_4$/AC) in Mg-air battery was found to hold specific discharge capacity of 962 mAh g^{-1} at current density of 40 mA cm^{-2}, which was higher than that of the bulk electrode (i.e.,782 mAh g^{-1}). The K_2NiF_4-type $La_{1.8}Sr_{0.2}CuO_4$ has been proved as a potential candidate for air cathode in Mg-air battery.

Keywords: $La_{1.8}Sr_{0.2}CuO_4$; K_2NiF_4-type; Mg-air battery; discharge capacity; cycle stability

1. INTRODUCTION

To satisfy the requirement of energy utilization and reduce the pollution of environment, the sustainable energy storage materials and devices have been developed [1-3]. Metal-air battery has been predicted to possess high theoretical energy density because of unlimited oxygen supplement from air in cathode [4-8]. Therefore, the capacitance of metal-air battery is only determined by negative metal. Metal-air battery has stable discharge voltage [9] and relatively high specific power density [5, 10]. Furthermore, the negative electrode of metal-air battery can be mechanically recharged (metal electrode replacement) to save the charging time [9]. Hence, the metal-air battery is considerable to be a good candidate to meet our energy needs.

Magnesium-air (Mg-air) battery has the highest theoretical open-circuit potential (3.09 V) among metal-air batteries family (aqueous system) [11] and very high theoretical energy density (6.8

kWh kg^{-1})[12]. Moreover, it is low cost and environmentally friendly (the electrolyte is NaCl aqueous solution). The electrochemical performance of Mg-air battery is mainly determined by the degree of oxygen reduction reaction (ORR) [12, 13]. Hence, the catalytic activity of cathode materials is the key factor [14]. The platinum-based materials have been proved to be the most efficient catalysts [15-17], however, it is rare and expensive. Therefore, to develop an economic catalyst is in need. A_2BO_4 with unique crystalline structure (K_2NiF_4-type structure, consisting of alternating layer of perovskite ABO_3 and AO rock-salt) are low cost, stable, nontoxic and with high catalytic activity [18, 19]. Where A is rare-earth metal (La), and B is transition metal (Mn, Co, Ni and Cu) [20, 21]. The A and B sites could be partially substituted with enhanced catalytic performance, since the substitution could help to distort the basic cubic crystalline structure and produce defects from oxygen vacancies[22]. The performance of perovskite-type catalysts is limited by the low conductivity and serious ohmic polarization[23]. K_2NiF_4-type La_2CuO_4 was studied because it has excellent electron conductivity, abundant oxygen vacancies and good catalytic activity[24, 25]. Furthermore, with partially substituted by Sr, the increased oxygen vacancies[26] and conductivity could be obtained as shown in previous works[25, 27-29].

In our study, with considering the annealing temperature and hydrothermal time, K_2NiF_4-type $La_{1.8}Sr_{0.2}CuO_4$ has been hydrothermal synthesized. The catalytic activity of $La_{1.8}Sr_{0.2}CuO_4$ for ORR was examined by studying the discharge behavior of Mg-air battery at relatively high current density (40 mA cm^{-2}). And also, the utility of active carbon as catalyst additive has been investigated. Field emission scanning electron microscopy (FESEM) was performed to determine the morphology of K_2NiF_4-type $La_{1.8}Sr_{0.2}CuO_4$. Electrochemical impedance studies (EIS) were utilized to testify the effect of synthesized condition and active carbon addition on the electron transfer of $La_{1.8}Sr_{0.2}CuO_4$ electrode.

2. EXPERIMENTAL

2.1 Chemicals

$Sr(NO_3)_2$ (99.5 %), $Cu(NO_3)_2{\cdot}3H_2O$ (99 %), $La(NO_3)_3{\cdot}6H_2O$ (99 %), KOH (95 %) and ethanol (99.5 %) were purchased from Aladdin Industrial Corporation. Polytetrafluoroethylene condensed liquid binder(PTFE, 60 wt%) and Super P conductive carbon black (CB) was from Shenzhen Kejing Star Technology Co., Ltd. Active carbon (specific surface area of 1000 m^2 g^{-1}, pore size distribution of 0.7-5 nm) was from Ningxia Xiangtaixin Material Technology Co., Ltd. Magnesium alloy AZ31B was from Dongguan Huitai Metal Materials Co., Ltd. All chemicals were used as received without any purification.

2.2 Preparation of $La_{1.8}Sr_{0.2}CuO_4$

0.2116 g $Sr(NO_3)_2$, 2.42 g $Cu(NO_3)_2{\cdot}3H_2O$ and 3.897 g $La(NO_3)_3{\cdot}6H_2O$ were dissolved in 50 ml ultrapure water with continues stirring. And then, 12 mol L^{-1} KOH was added to adjust pH to 13

and the volume to 75 mL. The above solution was sealed in a 100 mL Teflon autoclave and kept at 180 ℃ for 12 h, 48 h and 72 h respectively. The product was washed with ultrapure water for at least 3 times and dried at 60 ℃ for 12h. Finally, the heat treatment was carried out at 400 ℃ for 1h followed by temperature increasing to 650 ℃, 750 ℃ and 850 ℃ for 6 h, respectively.

2.3Preparation of Cathode

The synthesized $La_{1.8}Sr_{0.2}CuO_4$ was mixed with PTFE and CB in the mass ratio of 1:1:3, and it was used as the catalyst layer. The catalyst layer used nickel foam as current collector with working area of 1 cm^2. The $La_{1.8}Sr_{0.2}CuO_4$ with active carbon ($La_{1.8}Sr_{0.2}CuO_4$ /AC) catalyst layer was prepared by $La_{1.8}Sr_{0.2}CuO_4$, PTFE, carbon black (CB) and active carbon with the mass ratio of 1:1:2.4:0.6. The waterproof layer was made of 40 wt% PTFE and 60 wt% CB with ethanol addition. The cathode was consisted of catalyst layer, nickel foam and waterproof layer with a sandwiched structure.

2.4 Physical characterization

X-ray diffraction (XRD) patterns were recorded on a Shimadzu XRD6000 diffractometer with Cu-Kα as the radiation source (λ=0.154 nm). Field emission scanning electron microscopy (FESEM) was carried out with a Zeiss Sigma 500 microscope operated at 3 kV to determine the morphology $La_{1.8}Sr_{0.2}CuO_4$.

2.5 Electrochemical characterization

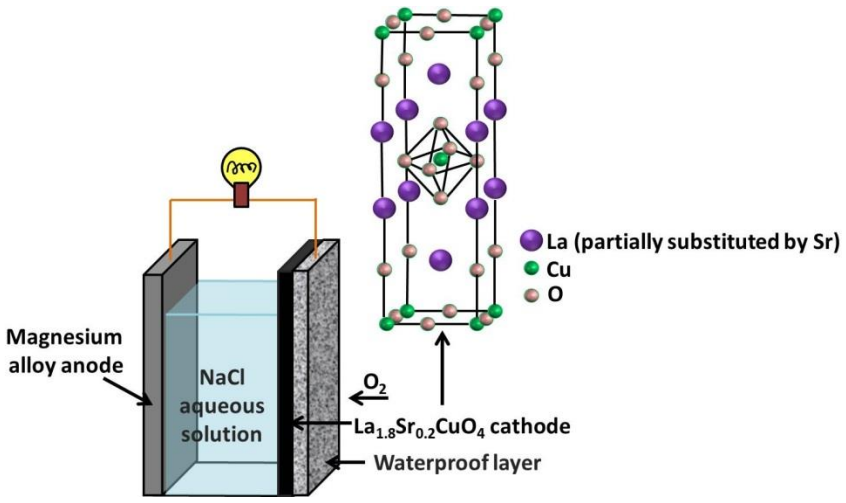

Figure 1 Schematic of Mg-air battery and the crystalline structure of $La_{1.8}Sr_{0.2}CuO_4$

The discharge performance of the Mg-air battery (consist of $La_{1.8}Sr_{0.2}CuO_4$ as cathode, magnesium alloy of AZ31B as anode and 20 wt% NaCl as aqueous solution) was analyzed via Neware battery testing system at the discharge current of 10 to100 mA cm^{-2} with 10 mA cm^{-2} interval. The schematic of Mg-air battery and the crystalline structure of $La_{1.8}Sr_{0.2}CuO_4$ are shown in Fig.1. The

operating life of the battery was also determined by Neware battery testing system at the discharge current of 40 mA cm^{-2} until AZ31B exhausted. The impedance spectroscopy of cathode was examined in a three-electrode system, a working electrode ($La_{1.8}Sr_{0.2}CuO_4$ air electrode), a platinum counter electrode and a Ag/AgCl reference electrode by using electrochemical workstation (CHI660e, Chenhua, China). The frequency was in the range of 100 kHz to 1 Hz at the initial potential of 0.2 V.

3. RESULTS AND DISCUSSION

Since $La_{1.8}Sr_{0.2}CuO_4$ is a potential candidate which could be used as the cathode in metal-air battery, the catalysis performance of $La_{1.8}Sr_{0.2}CuO_4$ should be further improved. Hence, the synthesized condition of $La_{1.8}Sr_{0.2}CuO_4$ needs to be optimized. In this study, the effect of hydrothermal time, annealing temperature and active carbon addition in $La_{1.8}Sr_{0.2}CuO_4$ has been discussed.

3.1 Effect of hydrothermal time

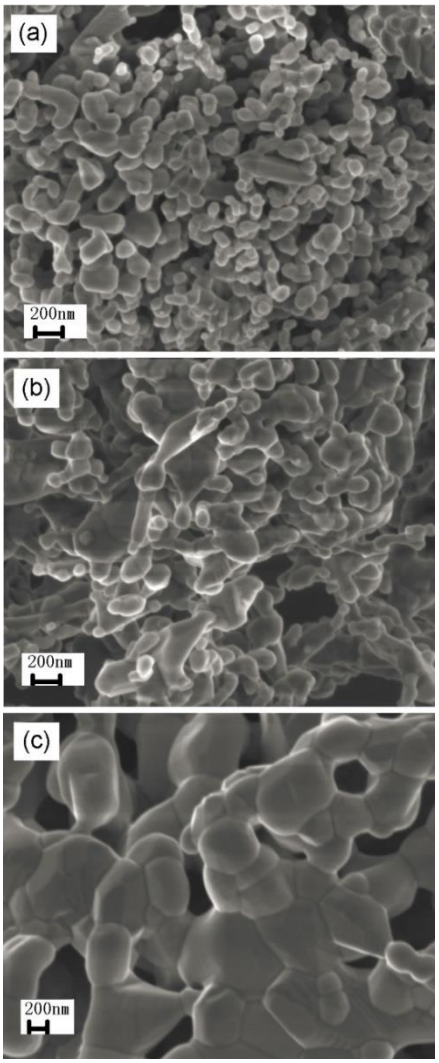

Figure 2 FESEM images of $La_{1.8}Sr_{0.2}CuO_4$ heat treated at 750 ℃ with hydrothermal time of 12 h (a), 48 h(b) and 72 h(c)

The FESEM images of the $La_{1.8}Sr_{0.2}CuO_4$ synthesized at various hydrothermal reaction time are shown in Fig. 2.

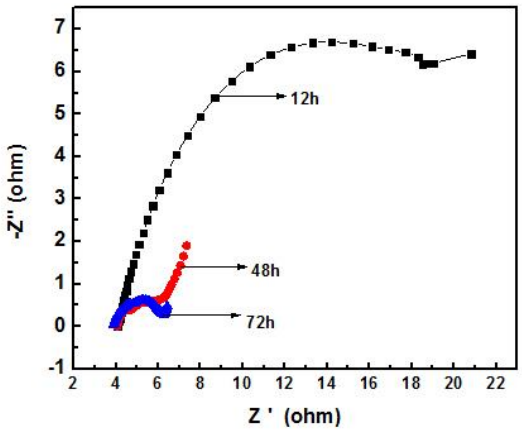

Figure 3 Nyquist plots of $La_{1.8}Sr_{0.2}CuO_4$ synthesized at hydrothermal time of 12 h, 48 h and 72 h with heat treatment temperature of 750 ℃.

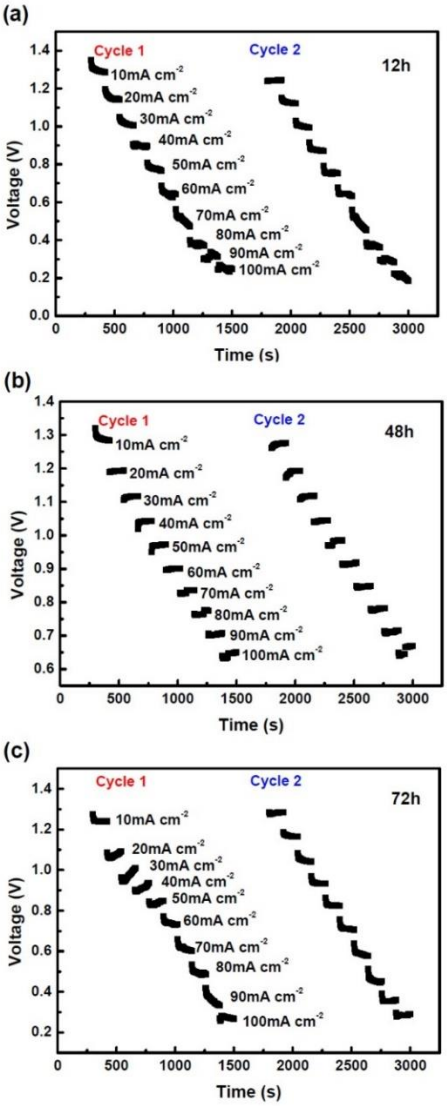

Figure 4 Cycle stability of $La_{1.8}Sr_{0.2}CuO_4$ synthesized at hydrothermal time of 12 h (a), 48 h (b) and 72 h (c) with heat treatment temperature of 750 ℃.

It is observed that primary particles of $La_{1.8}Sr_{0.2}CuO_4$ aggregate to form large-sized secondary particles. The size of secondary particles is around 80-200 nm, 200-400 nm and 400-600 nm corresponding to hydrothermal time of 12 h, 48 h and 72 h, respectively. It is clearly found that the size of secondary particles could continue to grow with the hydrothermal reaction time prolonging.

Fig.3 shows the electrochemical impedance (Nyquist plots) of $La_{1.8}Sr_{0.2}CuO_4$ synthesized at hydrothermal time of 12 h, 48 h and 72 h in 20 wt.% NaCl electrolyte. The measurements are conducted at the potential of 0.2 V. The solution resistances are similar (~4 Ω) for the $La_{1.8}Sr_{0.2}CuO_4$ at different hydrothermal time. The charge transfer resistances are around 20 Ω, 2.5 Ω and 2.5 Ω corresponding to the hydrothermal time of 12 h, 48 h and 72 h, respectively. It is found that both 48 h and 72 h $La_{1.8}Sr_{0.2}CuO_4$ have higher electron conductivity and catalytic activity as compared with 12 h one.

Discharge study has been performed in the assembled Mg-air battery at the current densities of 10 to 100 mA cm^{-2} with the interval of 10 mA cm^{-2}. Cycle stability measurement was carried out by using two discharge cycles at each current density for 2 min as shown in Fig.4. The discharging potential and the maximum power density of $La_{1.8}Sr_{0.2}CuO_4$ fabricated in the different conditions have been summarized in Table 1.

Table 1. Discharge potential and P_{max} of Mg-air battery for $La_{1.8}Sr_{0.2}CuO_4$ cathode fabricated at different conditions

Hydrothermal time (h)	Annealing temperature (℃)	Active carbon addition	Discharging potential (V) at 10 mA cm^{-2}	Discharging potential (V) at 100mA cm^{-2}	P_{max} (mW cm^{-2})
12（Cycle 1/Cycle 2）	750	N.A.	1.35/ 1.24	0.24/ 0.19	42.1
48（Cycle 1/Cycle 2）	750	N.A.	1.32/ 1.28	0.65/ 0.67	63.9
72（Cycle 1/Cycle 2）	750	N.A.	1.25/ 1.28	0.27/ 0.28	46.2
48（Cycle 1/Cycle 2）	650	N.A.	1.30/ 1.27	0.60/ 0.60	61.3
48（Cycle 1/Cycle 2）	850	N.A.	1.37/ 1.29	0.05/ 0.03	50.4
48（Cycle 1/Cycle 2）	750	Yes	1.36/ 1.28	0.70 / 0.71	70.5

For the $La_{1.8}Sr_{0.2}CuO_4$ synthesized at the hydrothermal time of 12 h (Fig. 4a), the discharge potential is 1.35 V and 0.24 V at the current density of 10 mA cm^{-2} and 100mA cm^{-2} in the discharge cycle 1. With the current density increasing, the discharge potential drops very fast. And in the discharge cycle 2, the discharge potential is 1.24 V and 0.19 V at current density of 10 mA cm^{-2} and 100 mA cm^{-2}, respectively. It has 110 mV drops at current density of 10 mA cm^{-2} and 50 mV drops at

current density of 100 mA cm^{-2}. It means the $La_{1.8}Sr_{0.2}CuO_4$ synthesized at hydrothermal time of 12 h is unstable as cathode.

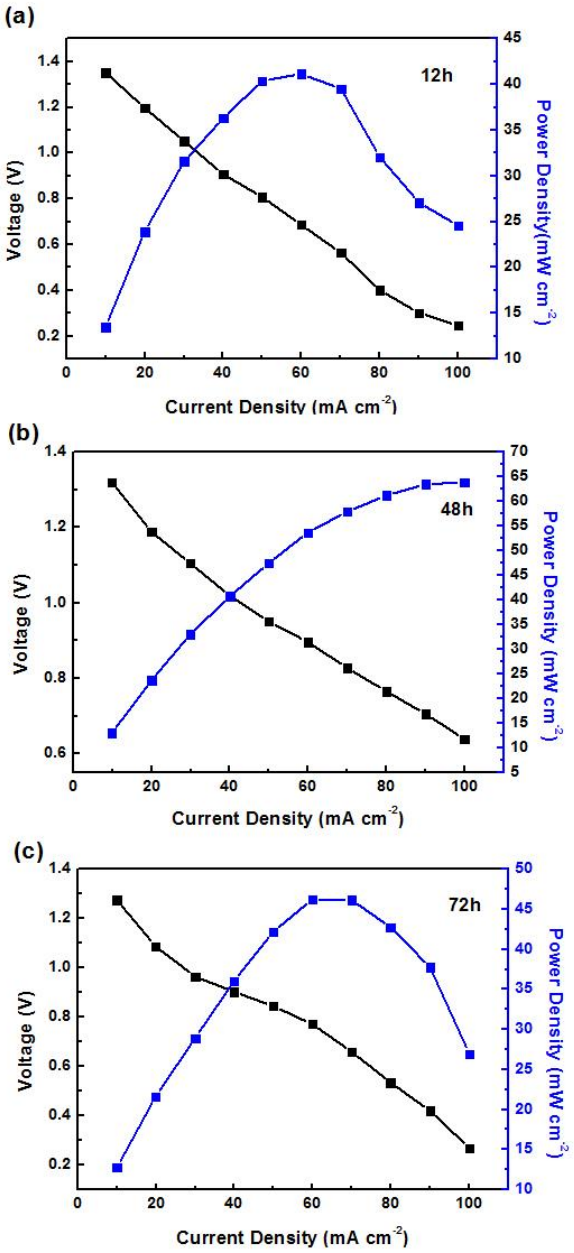

Figure 5. Current-Voltage-Power curves of $La_{1.8}Sr_{0.2}CuO_4$ synthesized at hydrothermal time of 12 h (a), 48 h (b) and 72 h (c) with heat treated temperature of 750 ℃.

For the $La_{1.8}Sr_{0.2}CuO_4$ synthesized at hydrothermal time of 72 h (Fig. 4c), as compared with the first discharge cycle, the discharge potentials of second cycle have 30 mV and 10 mV increase at current density of 10 mA cm^{-2} and 100 mA cm^{-2}. It indicates the $La_{1.8}Sr_{0.2}CuO_4$ synthesized at hydrothermal time of 72 h has a good stability as applied in Mg-air battery. But, the discharge potential still has a deep drop of 0.98 V from the current density of 10 mA cm^{-2} to 100 mA cm^{-2}. The $La_{1.8}Sr_{0.2}CuO_4$ synthesized at the hydrothermal time of 48 h (Fig. 4b) has discharging potential of 1.32 V and 0.65 V at the current density of 10 mA cm^{-2} and 100 mA cm^{-2} in the first cycle. The discharging

potential has 380 mV enhancement as compared with 72 h $La_{1.8}Sr_{0.2}CuO_4$ at the current density of 100 mA cm^{-2}. Furthermore, the discharge potential of second cycle has 20 mV enhancement at current density of 100 mA cm^{-2}. It means the $La_{1.8}Sr_{0.2}CuO_4$ synthesized at hydrothermal time of 48 h behaves good electrochemical stability and high-rate performance.

Fig. 5 shows Current-Voltage-Power curves of the $La_{1.8}Sr_{0.2}CuO_4$ synthesized at hydrothermal time of 12 h (a), 48 h (b) and 72 h (c). The maximum power density (P_{max}) of 42.1 mW cm^{-2}, 63.9 mW cm^{-2}, 46.2 mW cm^{-2} could be output as the cathode fabricated by the $La_{1.8}Sr_{0.2}CuO_4$ with the hydrothermal time of 12 h, 48 h and 72 h, respectively. The P_{max} of 48 h $La_{1.8}Sr_{0.2}CuO_4$ is the highest one among all synthesis condition. Although Nyquist measurement have shown the similar electron conductivity and resistance of the 48 h and 72 h ones, the $La_{1.8}Sr_{0.2}CuO_4$ synthesized at hydrothermal time of 48 h still has better catalytic activity than 72 h one. It could attribute to the size effect. Since the particle size of 48h one is smaller than that of 72h one, the 48h one has more active sites to facilitate catalytic reactions.

3.2 Effect of annealing temperature

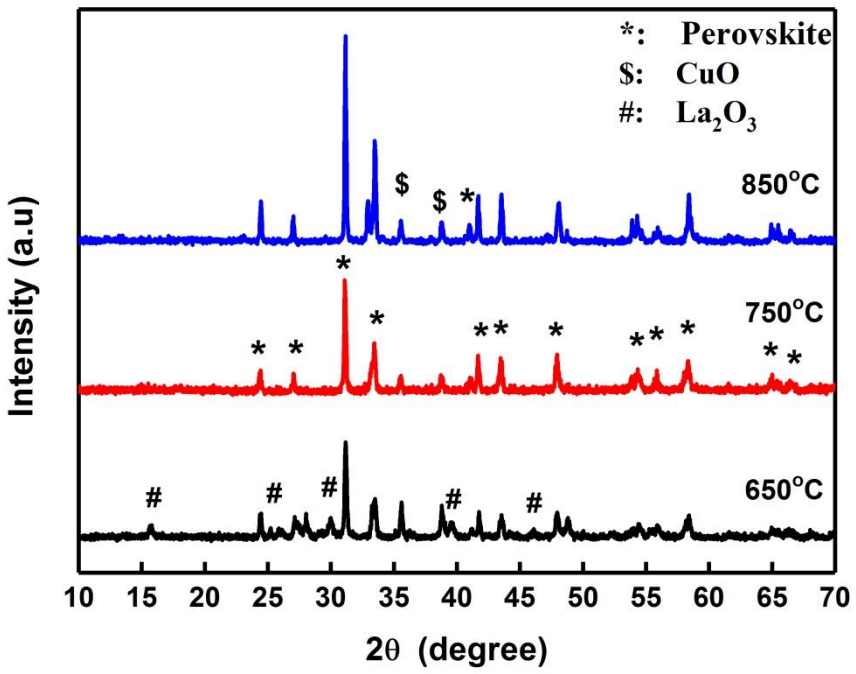

Figure 6. XRD patterns of $La_{1.8}Sr_{0.2}CuO_4$ at annealing temperature of 650 ℃, 750 ℃ and 850 ℃with hydrothermal time of 48 h.

The crystalline structure of $La_{1.8}Sr_{0.2}CuO_4$ fabricated at annealing temperature of 650 ℃, 750 ℃ and 850 ℃ was confirmed by XRD as shown in Fig 6. The main peaks can be assigned to the diffraction of $La_{1.8}Sr_{0.2}CuO_4$ (JCPDS No. 38-1427) [30].The impurity phase of CuO always presents in three samples. As the heat treatment temperature equals to 650 ℃, La_2O_3 exists due to uncompleted

reaction. With annealing temperature increased to 750 ℃ and even higher, the diffraction peaks of $La_{1.8}Sr_{0.2}CuO_4$ became sharper, and the peaks generated from La_2O_3 will disappear.

The Nyquist plots of $La_{1.8}Sr_{0.2}CuO_4$ fabricated at annealing temperature of 650 ℃, 750 ℃ and 850 ℃ have been shown in Fig.7. The measurements were conducted at potential of 0.2 V. The solution resistances of the $La_{1.8}Sr_{0.2}CuO_4$ cathodes are 4.3 Ω, 4.0 Ω and 4.6 Ω corresponding to the annealing temperature of 650 ℃, 750 ℃ and 850 ℃, respectively. The charge transfer resistances are around 1.7 Ω, 2.5 Ω and 1.9 Ω corresponding to annealing temperature of 650 ℃, 750 ℃ and 850 ℃. Combined the solution resistance and the charge transfer resistance, the cathode materials annealed at three different temperatures have the similar electron conductivity upon Nyquist testing.

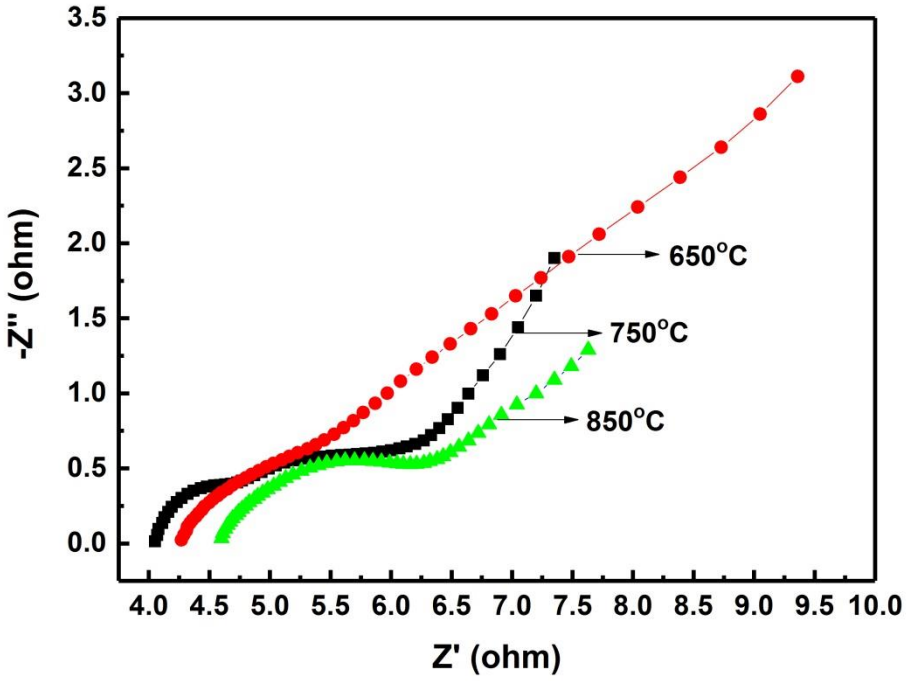

Figure 7. Nyquist plots of $La_{1.8}Sr_{0.2}CuO_4$ synthesized at annealing temperature of 650 ℃, 750 ℃ and 850 ℃ with hydrothermal time of 48 h.

Fig.8 shows the cycle stability test which was carried out in two cycles at each current density for 2 min. In the discharge cycle 1, the $La_{1.8}Sr_{0.2}CuO_4$ synthesized at the annealing temperature of 650 ℃, 750 ℃ and 850 ℃ have the discharge potential of 1.30 V, 1.32 V and 1.37 V at the current density of 10 mA cm^{-2}, respectively. It means the working potential increases with the annealing temperature. At the second discharge cycle, the discharge potentials drop to 1.27 V, 1.28 V and 1.29 V, individually, corresponding to 30 mV, 40 mV and 80 mV drops. With current density increased to 100 mA cm^{-2}, the discharge potential is 0.60 V, 0.65 V and 0.05 V at current density of 100 mA cm^{-2}, respectively. The $La_{1.8}Sr_{0.2}CuO_4$ heat treated at 850 ℃ has been shown the worst catalytic activity due to its rapid drops of discharge potential at each current density in 2 min interval. The discharge potential of 650 ℃ and 750 ℃ $La_{1.8}Sr_{0.2}CuO_4$ at the considering current density has no drops even at the second cycle. As compared with the $La_{1.8}Sr_{0.2}CuO_4$ treated at 650 ℃, the discharge potential of

catalyst treated at 750 ℃ has 50 mV increases. It indicates the $La_{1.8}Sr_{0.2}CuO_4$ synthesized at annealing temperature of 750ºC has the highest cycle stability and the best high-rate performance. Current-Voltage-Power curves of $La_{1.8}Sr_{0.2}CuO_4$ synthesized at annealing temperature of 650 ℃ (a), 750 ℃ (b) and 850 ℃ (c) are shown in Fig. 9.

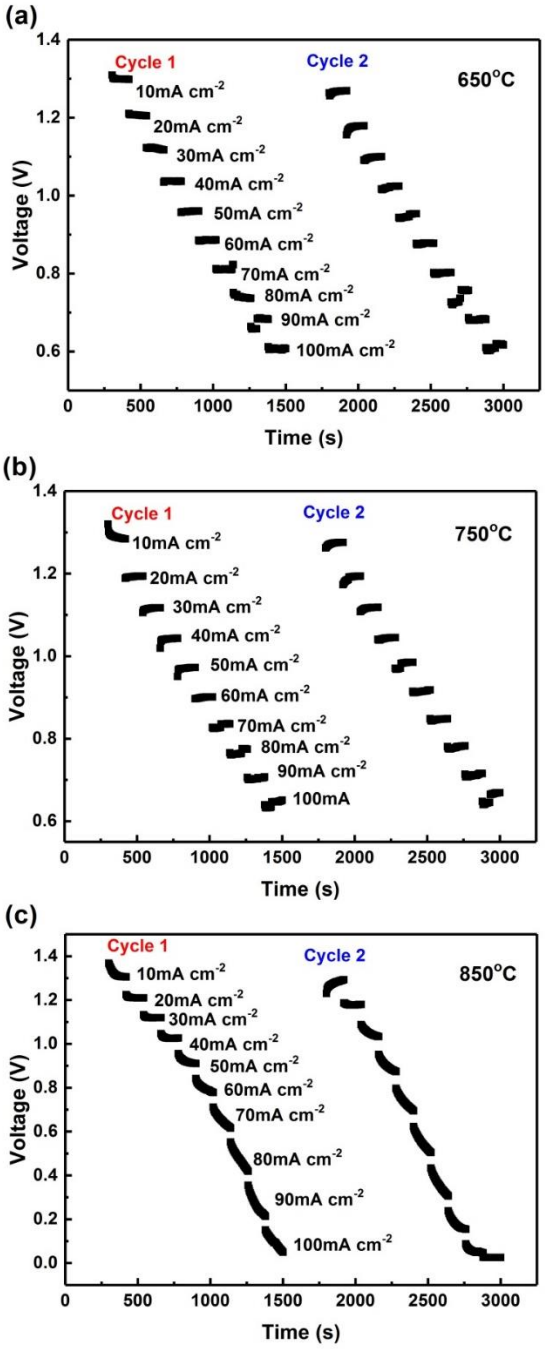

Figure 8. Cycle stability of $La_{1.8}Sr_{0.2}CuO_4$ synthesized at annealing temperature of 650 ℃, 750 ℃ and 850 ℃ with hydrothermal time of 48 h.

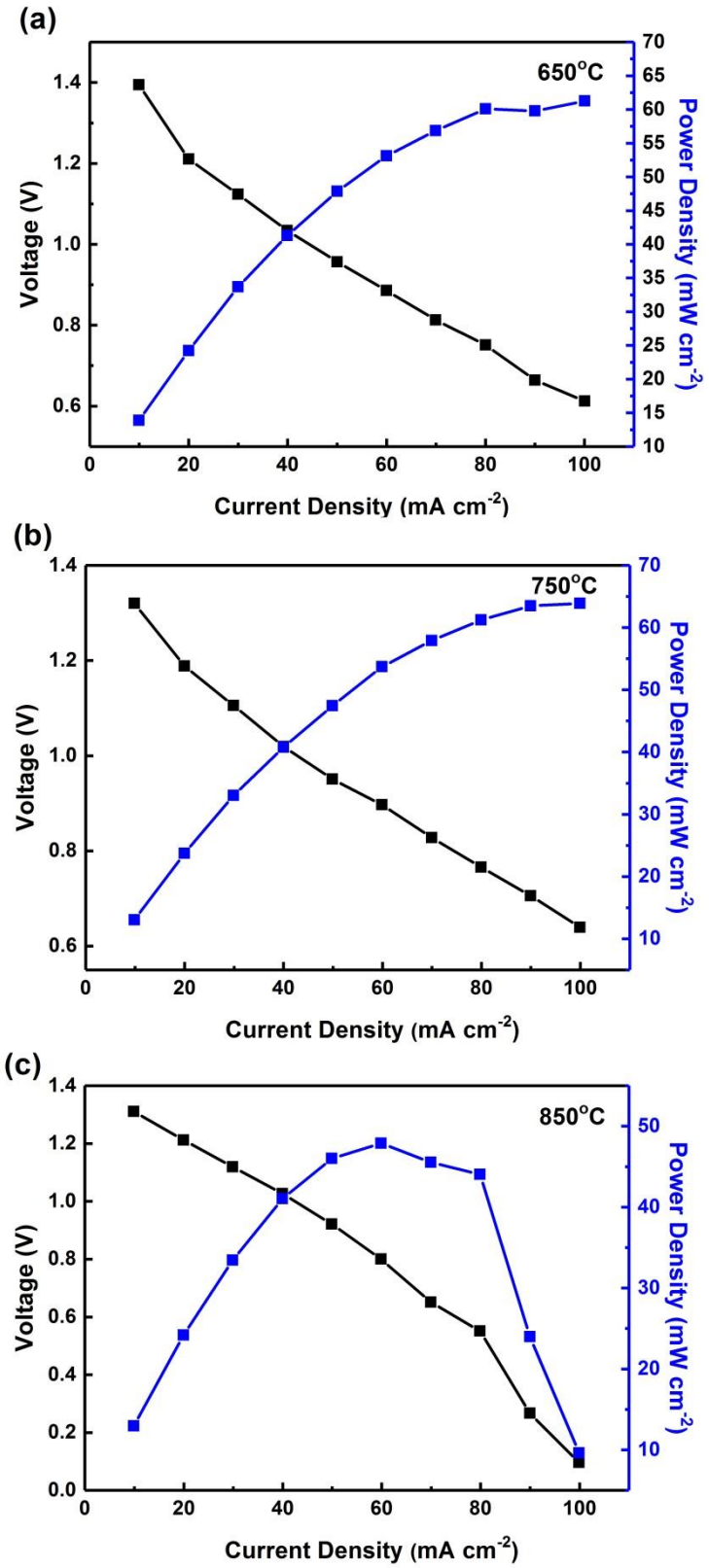

Figure 9. Current-Voltage-Power curves of $La_{1.8}Sr_{0.2}CuO_4$ synthesized at annealing temperature of 650 ℃ (a), 750 ℃ (b) and 850 ℃ (c) with hydrothermal time of 48 h.

The $La_{1.8}Sr_{0.2}CuO_4$ cathodes with annealing temperature of 650 ℃, 750 ℃ and 850 ℃ applied in Mg-air battery have P_{max} of 61.3 mW cm^{-2}, 63.9 mW cm^{-2} and 50.4 mW cm^{-2}, respectively. The

$La_{1.8}Sr_{0.2}CuO_4$ treated at 750 ℃ has the highest P_{max}. Considering the time effect of the hydrothermal reaction, the $La_{1.8}Sr_{0.2}CuO_4$ with the hydrothermal time of 48 h and the annealing temperature of 750 ℃ has the relatively high electron conductivity and catalytic activity.

3.3 Effect of active carbon addition

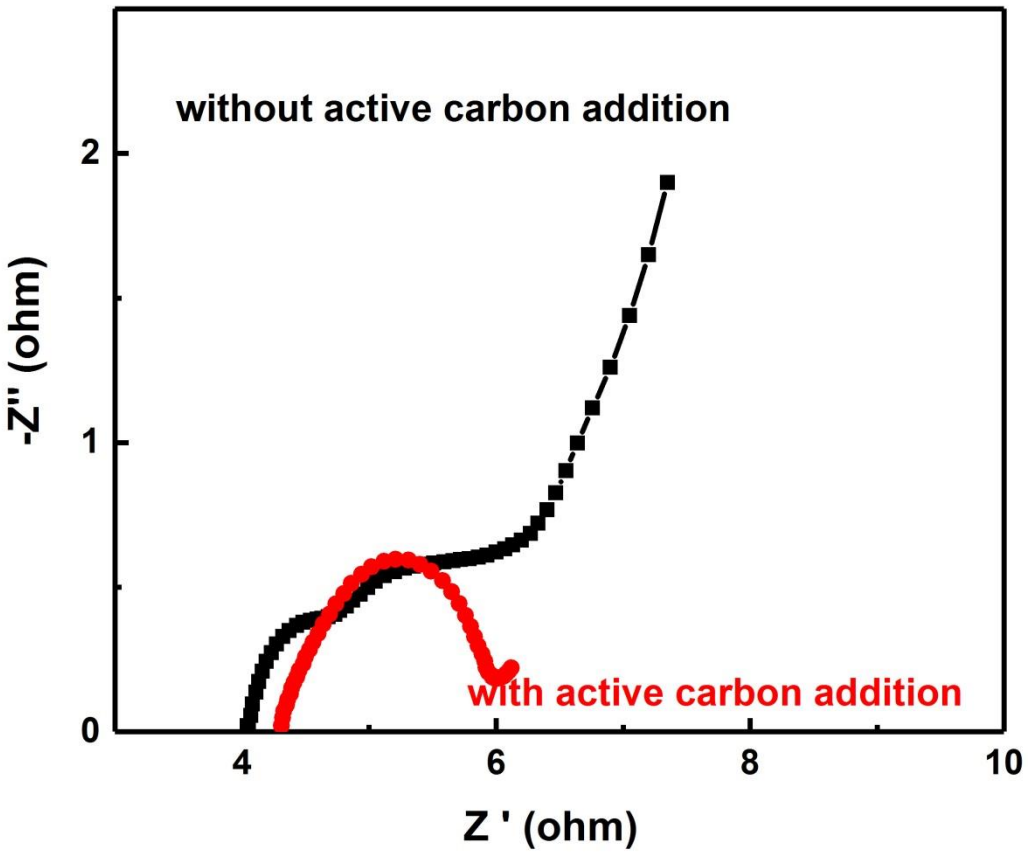

Figure 10. Nyquist plots of $La_{1.8}Sr_{0.2}CuO_4$ with and without active carbon heat treated at 750 ℃ with the hydrothermal time of 48 h.

As shown in Fig.10, the solution resistances of the $La_{1.8}Sr_{0.2}CuO_4$ cathodes with and without carbon addition are 4.3 Ω and 4.0 Ω. The charge transfer resistances are around 1.7 Ω and 2.5 Ω, respectively. It manifests that the electron transfer capability of the $La_{1.8}Sr_{0.2}CuO_4$ with active carbon addition is relatively good. As compared with bulk ones synthesized at various hydrothermal and heat treatment temperatures, the $La_{1.8}Sr_{0.2}CuO_4$/AC has the lowest resistance. It results in the good catalytic performance of the cathode. This is consistent with the reported literatures that materials with carbon-based supporting have enhanced conductivity as compared with bulk ones [20, 31-33].

The discharge cycle stability characterization of the $La_{1.8}Sr_{0.2}CuO_4$ cathodes with and without active carbon was carried out by the battery testing system as shown in Fig. 11. The $La_{1.8}Sr_{0.2}CuO_4$ with active carbon addition ($La_{1.8}Sr_{0.2}CuO_4$/AC) has 80 mV drops with the initial discharging potential of 1.37 V at the current density of 10 mA cm^{-2}. And at the current density of 100 mA cm^{-2}, there are no any drops with discharge potential of 0.7 V and the discharge potential of $La_{1.8}Sr_{0.2}CuO_4$/AC has 50

mV enhancement as compared with the bulk one. Current-Voltage-Power curves of bulk $La_{1.8}Sr_{0.2}CuO_4$ and $La_{1.8}Sr_{0.2}CuO_4$/AC are shown in Fig. 12. The P_{max} of the $La_{1.8}Sr_{0.2}CuO_4$/AC is 70.5 mW cm^{-2}, it is about 10.3 % higher comparing with P_{max} of the bulk $La_{1.8}Sr_{0.2}CuO_4$. $La_{1.8}Sr_{0.2}CuO_4$ has been proved with good conductivity previously as utilized in high temperature fuel cells [27, 28, 30]. In this study, the good conductivity of $La_{1.8}Sr_{0.2}CuO_4$ is further verified as applied in cathode of Mg-air battery at room temperature, which indicates the $La_{1.8}Sr_{0.2}CuO_4$ is a potential candidate of catalyst for oxygen reduction reaction. Moreover, the catalytic activity of $La_{1.8}Sr_{0.2}CuO_4$ cathodes is improved with active carbon addition. The microporous and mesoporous structure of the active carbon could help to disperse the catalysts and stabilize the electrode efficiently.

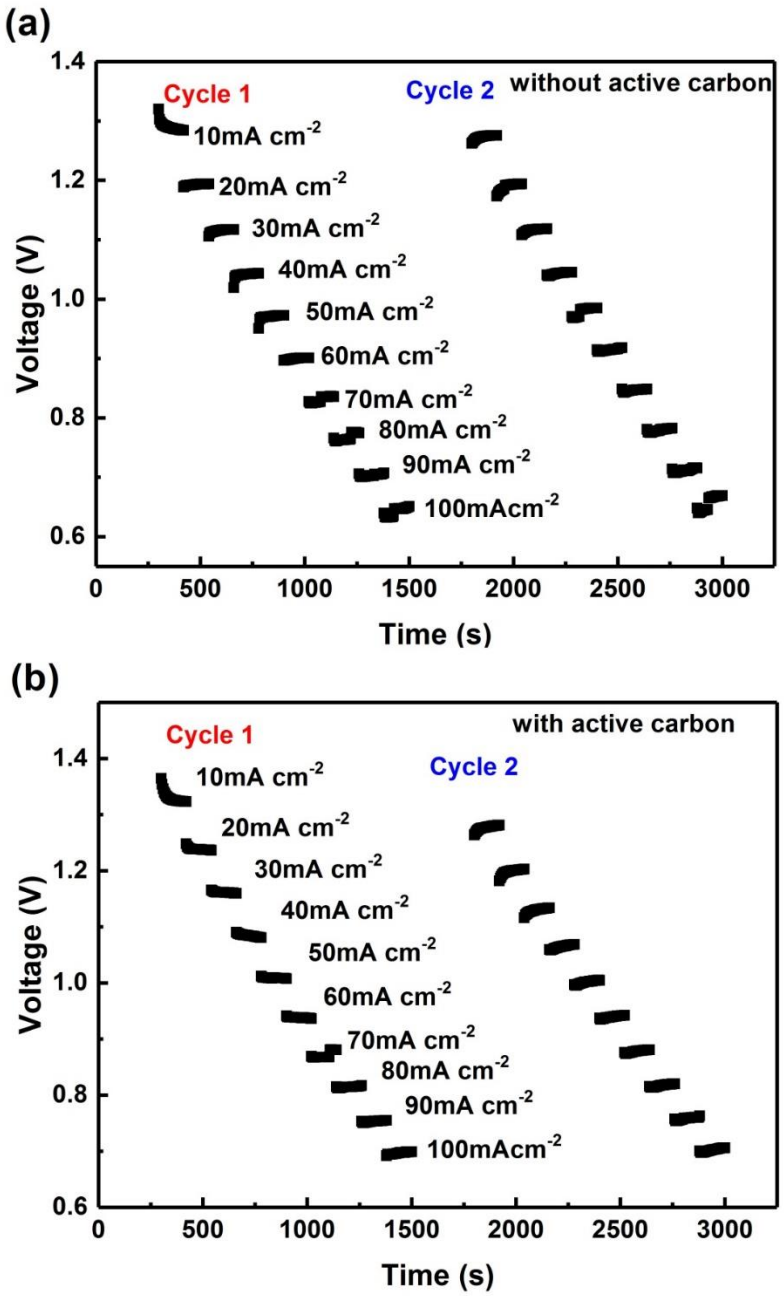

Figure 11. Discharge performance of $La_{1.8}Sr_{0.2}CuO_4$ without (a) and with (b) active carbon heat treated at 750 ℃ with hydrothermal time of 48 h.

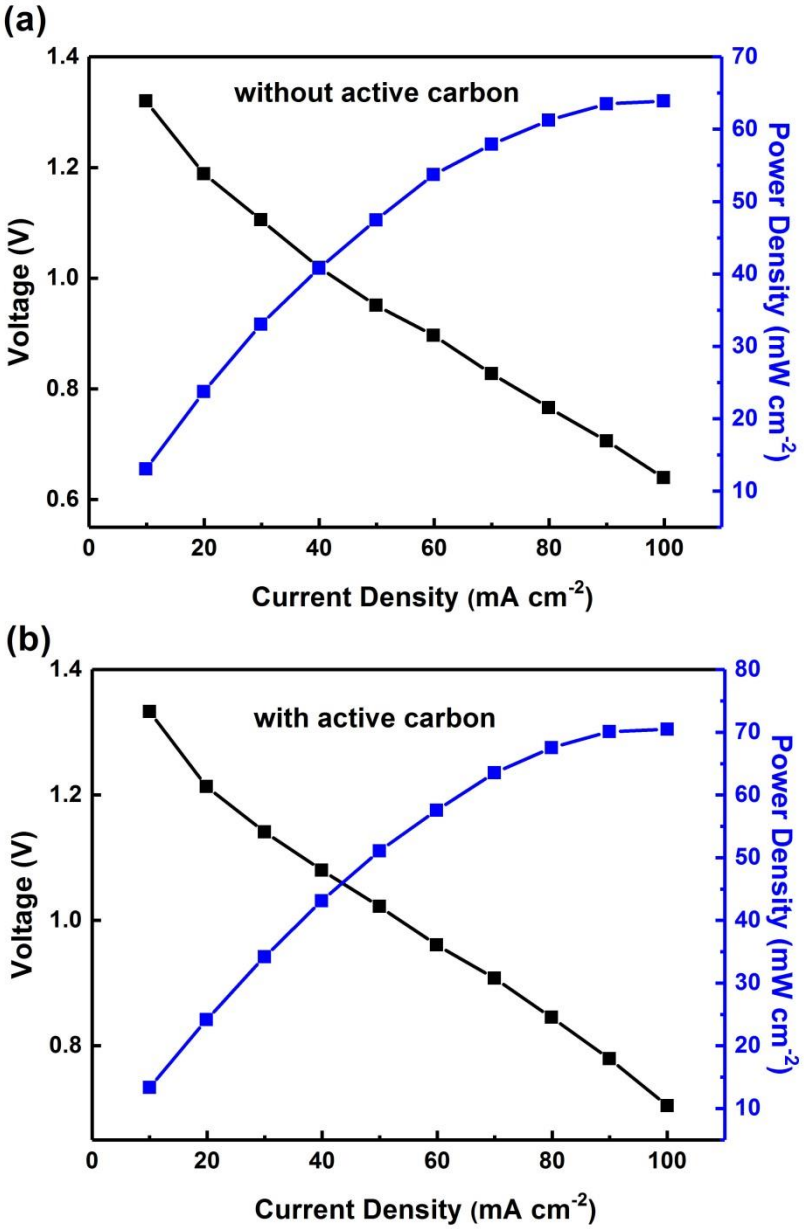

Figure 12. Current-Voltage-Power curves of $La_{1.8}Sr_{0.2}CuO_4$ without (a) and with (b) active carbon heat treated at 750 ℃ with hydrothermal time of 48 h.

The battery life of the bulk $La_{1.8}Sr_{0.2}CuO_4$ and the $La_{1.8}Sr_{0.2}CuO_4$/AC were measured at the current density of 40 mA cm^{-2} as shown in Fig. 13. The open-circuit voltage obtained from the bulk $La_{1.8}Sr_{0.2}CuO_4$ and the $La_{1.8}Sr_{0.2}CuO_4$/AC was 1.5 and 1.48 V, respectively. As observed from the discharge curves, $La_{1.8}Sr_{0.2}CuO_4$/AC cathode exhibits elongated discharge plateau as compared with the bulk $La_{1.8}Sr_{0.2}CuO_4$. The rapid drop in voltage could be observed in both cathodes due to the Mg alloy exhausted. The battery life is 12 h and 10.8 h corresponding to the $La_{1.8}Sr_{0.2}CuO_4$ with and without AC addition. The $La_{1.8}Sr_{0.2}CuO_4$/AC cathode achieved the discharge capacity of 962 mAh g^{-1} (evaluated by mass of AZ31B consumption) compared to 782 mAh g^{-1} obtained from the bulk $La_{1.8}Sr_{0.2}CuO_4$ based cathode. As an additive, the active carbon enhanced the electrical conductivity in cathode, resulting in the obvious improvement of the battery discharge performance.

Table 2. Comparison of cathodic catalysts reported in the literatures

Cathode material	References	Electrolyte	Power density (mW cm^{-1})	Operating voltage (V)	Specific capacity (mAh g^{-1})
PdSn/MWCNTs	[34]	10 wt.% NaCl	112.4	1.23 at 40 mA cm^{-2}	-
PPcFe/C	[35]	10 wt.% NaCl	50.5	1.10 at 30 mA cm^{-2}	-
MnO_2/CNTs-OH	[31]	15 wt.% NaCl	79.2	1.13 at 30 mA cm^{-2}	-
MnO_2/C	[31]	15 wt.% NaCl	63	1.10 at 30 mA cm^{-2}	-
α-MnO_2 nanowires	[32]	10 wt.% KCl	66	1.18 at 30 mA cm^{-2}	-
α-MnO_2 nanowires/graphene	[32]	10 wt.% KCl	96	1.20 at 30 mA cm^{-2}	-
MnO_2/MWCNTs	[33]	10 wt.% NaCl	70.47	1.20 at 30 mA cm^{-2}	-
MnO_2/C	[33]	10 wt.% NaCl	60.95	1.15 at 30 mA cm^{-2}	-
Pd/XC-72	[36]	2 M NaCl	68	1.30 at 30 mA cm^{-2}	-
PdCo/C	[37]	10 wt.% NaCl	200	1.20 at 30 mA cm^{-2}	-
RGO/Mn_3O_4	[38]	3.5 wt.% NaCl	-	0.95 at 10 mA cm^{-2}	163
carbon fiber felt	[39]	10 wt.% NaCl	116	1.10 at 30 mA cm^{-2}	-
Ag-Co_3O_4@N-doped carbon/CNTs	[40]	10 wt.% KCl	88.9	1.15 at 30 mA cm^{-2}	-
$SmMn_2O_{4.86}$	[41]	1 M NaCl	101	1.15 at 30 mA cm^{-2}	1770
$La_{1.8}Sr_{0.2}CuO_4$/AC	Our work	20 wt.% NaCl	70.5	1.32 at 10 mA cm^{-2}	962
				1.16 at 30 mA cm^{-2}	

Table 2 shows the electrolyte, power density, operating voltage and specific capacity of Mg-air battery obtained from the literature of the precious metal and nonprecious materials compared with our synthesized $La_{1.8}Sr_{0.2}CuO_4$/AC cathode. Normally, the specific capacity of Mg-air battery is evaluated by Mg anode consumption. Hence, for the cathode study, the specific capacity is seldom calculated. 962 mAh g^{-1} obtained in our study is relatively high value for Mg-air battery, although it is not the highest among all reported ones. $La_{1.8}Sr_{0.2}CuO_4$/AC shows relatively high power density as compared with other nonprecious materials. Moreover, the power density of $La_{1.8}Sr_{0.2}CuO_4$/AC is even higher than that of noble catalyst of Pd/XC-72 [36]. As the substrate was replaced by CNTs or graphene, the power density has an apparent enhancement as shown in ref.[31], [33] and [34]. In the recent study of nonprecious $SmMn_2O_{4.86}$ [41], it shows the excellent performance for Mg-air battery application. Not only the power density, but also the specific capacity is competitive. In the comparisons of operating voltage, it obeys the same rule that the noble metal-based cathode can reach the higher voltage. However, there is only a slight difference of 40-50 mV between noble and non-noble ones. Although there are so many testing issues should be considered, it is apparently that the noble metal catalyst could be replaced by nonprecious one in some days of the not far future. $La_{1.8}Sr_{0.2}CuO_4$/AC we fabricated is a novel candidate for air cathode, it has been proved with moderate performance in our study. With adjusting the ratio between La and Sr, or replacing Sr or Cu by the other elements, or

designing the special structure of final products, we believe the performance of air electrode will have a great improvement.

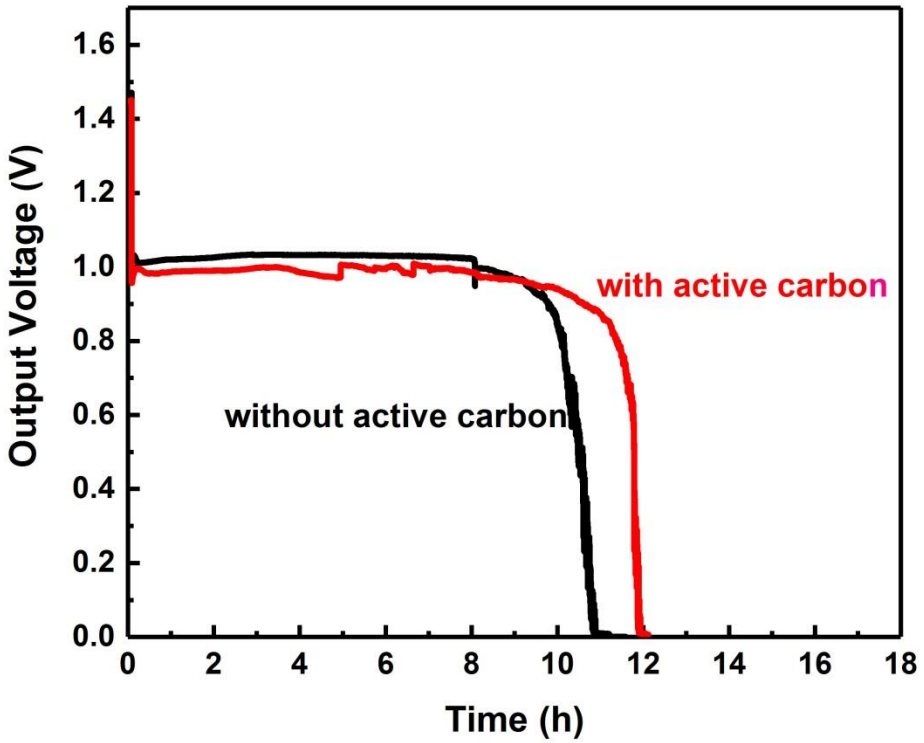

Figure 13 Discharge life of Mg-air battery with and without active carbon at current density of 40mA cm^{-2}.

4. CONCLUSION

The K_2NiF_4-type $La_{1.8}Sr_{0.2}CuO_4$ was hydrothermal synthesized in this study. And its utilization in magnesium-air battery has been explored. The optimized fabrication condition of $La_{1.8}Sr_{0.2}CuO_4$ has been determined. As the hydrothermal time of 48h and annealing temperature of 750 ℃, the K_2NiF_4-type $La_{1.8}Sr_{0.2}CuO_4$ is with discharge potential of 1.32 V and 0.65 V at current density of 10 mA cm^{-2} and 100 mA cm^{-2}, respectively, and has discharging capacity of 782 mAh g^{-1}. Furthermore, the $La_{1.8}Sr_{0.2}CuO_4$ cathode with active carbon addition for Mg-air battery has been studied. The discharge potential at current density of 100 mA cm^{-2} could be improved to 0.70 V. The active carbon based cathode in Mg-air battery achieved maximum discharge capacity (962 mAh g^{-1}), which was 18 % higher than that of the bulk one. Likewise, the active carbon raised the Mg-air battery life in hours up to 15 %. As a result, the K_2NiF_4-type $La_{1.8}Sr_{0.2}CuO_4$ could be a potential candidate utilized in cathode of Mg-air battery.

ACKNOWLEDGEMENT
This study is supported by West Light Foundation of The Chinese Academy of Sciences (XAB2019AW09), Research Project of Ningxia Colleges and Universities (NGY2015159), Natural Science Foundation of Ningxia Province (NZ16091, 2019AAC03114), and National Natural Science Foundation of China (NSFC, 21563001).

References

1. C. Daniel, J.O. Besenhard, Wiley-VCH, Oak Ridge, 2011.
2. J. Pan, X.L. Tian, S. Zaman, Z. Dong, H. Liu, H.S. Park, B.Y. Xia, *Batteries & Supercaps*, 2 (2019) 336.
3. Q. Liu, Z. Chang, Z. Li, X. Zhang, *Small Methods*, 2 (2018) 1700231.
4. R. Cao, J.-S. Lee, M. Liu, J. Cho, *Adv. Energy Mater.*, 2 (2012) 816.
5. Y. Li, J. Lu, *ACS Energy Lett.*, 2 (2017) 1370.
6. D. Zhou, Y. Jia, H. Yang, W. Xu, K. Sun, J. Zhang, S. Wang, Y. Kuang, B. Liu, X. Sun, *J. Mater. Chem. A*, 6 (2018) 21162.
7. H. Luo, W.-J. Jiang, Y. Zhang, S. Niu, T. Tang, L.-B. Huang, Y.-Y. Chen, Z. Wei, J.-S. Hu, *Carbon*, 128 (2018) 97.
8. P. Da, M. Wu, K. Qiu, D. Yan, Y. Li, J. Mao, C. Dong, T. Ling, S. Qiao, *Chem. Eng. Sci.*, 194 (2019) 127.
9. M. Mayilvel Dinesh, K. Saminathan, M. Selvam, S.R. Srither, V. Rajendran, K.V.I.S. Kaler, *J. Power Sources*, 276 (2015) 32.
10. L. Wei, H.E. Karahan, S. Zhai, H. Liu, X. Chen, Z. Zhou, Y. Lei, Z. Liu, Y. Chen, *Adv. Mater.*, 29 (2017) 1701410.
11. Y. Xue, H. Miao, S. Sun, Q. Wang, S. Li, Z. Liu, *J. Power Sources*, 297 (2015) 202.
12. J.-G. Zhang, P.G. Bruce, X.G. Zhang, Metal–Air Batteries, Handbook of Battery Materials, Wiley-VCH Verlag GmbH & Co. KGaA, 2011, pp. 757.
13. X. Cai, L. Lai, J. Lin, Z. Shen, *Materials Horizons*, (2017).
14. F. Cheng, J. Chen, *Chem. Soc. Rev.*, 41 (2012) 2172.
15. A. Mahata, P. Bhauriyal, K.S. Rawat, B. Pathak, *ACS Energy Lett.*, 1 (2016) 797.
16. A.L. Strickler, A. Jackson, T.F. Jaramillo, *ACS Energy Lett.*, 2 (2017) 244.
17. J. Gao, J. Zou, X. Zeng, W. Ding, *RSC Adv.*, 6 (2016) 83025.
18. J.M. Longo, P.M. Raccah, *J. Solid State Chem.*, 6 (1973) 526.
19. N. Guilhaume, S.D. Peter, M. Primet, *Applied Catalysis B: Environmental*, 10 (1996) 325.
20. N.-I. Kim, R.A. Afzal, S.R. Choi, S.W. Lee, D. Ahn, S. Bhattacharjee, S.-C. Lee, J.H. Kim, J.-Y. Park, *J. Mater. Chem. A*, 5 (2017) 13019.
21. A.G. Bhavani, W.Y. Kim, J.S. Lee, *ACS Catalysis*, 3 (2013) 1537.
22. Y. Wu, Z. Zhao, Y. Liu, X. Yang, *J. Mol. Catal. A: Chem.*, 155 (2000) 89.
23. G. Yang, C. Su, R. Ran, M.O. Tade, Z. Shao, *Energy & Fuels*, 28 (2014) 356.
24. M.I. Houchati, M. Ceretti, C. Ritter, W. Paulus, *Chem. Mater.*, 24 (2012) 3811.
25. X. Cai, L. Lai, J. Lin, Z. Shen, *Mater. Horiz.*, 4 (2017) 945.
26. Y. Wang, F. Baiutti, G. Gregori, G. Cristiani, U. Salzberger, G. Logvenov, J. Maier, P.A. van Aken, *ACS Appl. Mater. Interfaces*, 8 (2016) 6763.
27. J. Zhu, Z. Zhao, D. Xiao, J. Li, X. Yang, Y. Wu, *J. Mol. Catal. A: Chem.*, 238 (2005) 35.
28. G.N. Mazo, S.N. Savvin, E.V. Mychka, Y.A. Dobrovol'skii, L.S. Leonova, *Russ. J. Electrochem.*, 41 (2005) 448.
29. G.N. Mazo, O.A. Shlyakhtin, S.N. Savvin, *Int. J. Inorg. Mater.*, 3 (2001) 31.
30. F. Teng, B. Gaugeu, S. Liang, Y. Zhu, *Applied Catalysis A: General*, 328 (2007) 156.
31. Z. Zhang, Z. Li, C. Sun, T. Zhang, S. Wang, *Catal. Today*, 298 (2017) 241.
32. M. Jiang, H. He, C. Huang, B. Liu, W.-J. Yi, Z.-S. Chao, *Electrochim. Acta*, 219 (2016) 492.
33. P. Yue, Z. Li, S. Wang, Y. Wang, *Int. J. Hydrogen Energy*, 40 (2015) 6809.
34. C. Zhao, Y. Jin, W. Du, C. Ji, X. Du, *J. Electroanal. Chem.*, 826 (2018) 217.
35. Z. Li, J. Yang, G. Xu, S. Wang, *J. Power Sources*, 242 (2013) 157.
36. W. Yang, S. Yang, J. Guo, G. Sun, Q. Xin, *Carbon*, 45 (2007) 397.
37. C. Zhao, X. Yan, G. Wang, Y. Jin, X. Du, W. Du, L. Sun, C. Ji, *Int. J. Hydrogen Energy*, 43 (2018) 5001.

38. J. Ma, C. Qin, Y. Li, F. Ren, Y. Liu, G. Wang, *J. Power Sources*, 430 (2019) 244.
39. C. Shu, E. Wang, L. Jiang, G. Sun, *Int. J. Hydrogen Energy*, 38 (2013) 5885.
40. M. Jiang, H. He, W.-J. Yi, W. Huang, X. Pan, M.-Y. Wang, Z.-S. Chao, *Electrochem. Commun.*, 77 (2017) 5.
41. X. Zhao, L. Wang, X. Chen, W. Wang, H.L. Xin, X. Du, J. Yang, *J. Power Sources*, 449 (2020) 227482